Fermi National Accelerator Laboratory

FERMILAB-Conf-90/85-E
[E-741/CDF]

The Dijet Invariant Mass at the Tevatron Collider*

The CDF Collaboration

presented by

Paola Giannetti
Instituto Nazionale di Fisica Nucleare
Pisa, Italy

May 9, 1990

* Presented at the XXVth Rencontres de Moriond, Les Arcs, France, March11-17, 1990.

Operated by Universities Research Association Inc. under contract with the United States Department of Energy

CDF/PUB/JET/PUBLIC/1177
CONF 90/85-E
May 9, 1990

THE DIJET INVARIANT MASS AT THE TEVATRON COLLIDER

CDF Collaboration*
Presented by Paola Giannetti
Istituto Nazionale di Fisica Nucleare
Pisa, ITALY

ABSTRACT

The differential cross section of the process p + pbar → jet + jet + X as a function of the dijet invariant mass has been measured with the CDF detector[1] at a center of mass energy of 1.8 TeV at the Tevatron Collider in Fermilab. The present analysis is based on the sample of events collected in the 1988/89 run, amounting to a total integrated luminosity of 4.2 pb^{-1}. A comparison to leading order QCD and quark compositeness predictions is presented as well as a study of the sensitivity of the mass spectrum to the gluon radiation.

* The CDF collaboration
Argonne National Laboratory - Brandeis University -
University of Chicago - Fermi National Accelerator Laboratory -
Istituto Nazionale di Fisica Nucleare, Laboratori Nazionali di Frascati -
Harvard University - University of Illinois -
National Laboratory for High Energy Physics (KEK) -
Lawrence Berkeley Laboratory - University of Pennsylvania -
Istituto Nazionale di Fisica Nucleare, University and Scuola Normale Superiore of Pisa -
Purdue University - Rockefeller University - Rutgers University - Texas A&M University -
University of Tsukuba - Tufts University - University of Wisconsin

Pub. Proceedings XXVth Rencontres de Moriond, Les Arcs, Savoie, France,
March 11-17, 1990

1. INTRODUCTION

The interest for the measurement of the dijet mass spectrum is manifold.

a) It constitutes an important check of the QCD theoretical predictions and a probe for the possible internal structure of the quarks[2].

b) New physics can show up as resonance bumps in the mass spectrum or, for negative results, limits can be defined on the mass of new particles as in the case of the axigluon[3].

c) A detailed study of the dependence of the mass spectrum on the number of jets helps in the difficult issue of analyzing the characteristics of gluon radiation in the parton-parton scattering process.

2. THE DIJET MASS SPECTRUM

2.1 Trigger:

The events used in the analysis come from the JET_20, JET_40, and JET_60 online triggers in the 1988/89 run of the CDF experiment. These triggers basically require the presence of at least one energy cluster in the calorimeter with a transverse energy greater than, respectively, 20, 40, and 60 GeV.

2.2 Clustering Algorithm

The clustering algorithm[4], which exploits the projective tower geometry of the CDF calorimeter, produces a list of energy clusters. It uses the following parameters:

- Cone radius $R = (\Delta\varphi^2 + \Delta\eta^2)^{1/2} = 0.7$ (the radius of the region where the calorimeter energy is integrated).
- Tower threshold $E_{thr} = 0.2$ GeV (the energy threshold for a calorimeter tower to enter the cluster energy sum).
- Seed tower threshold $E_{seed} = 1$ GeV (threshold for a tower to initiate the cluster search).

The algorithm also gives the momentum of each cluster, assuming a massless particle for each calorimeter tower belonging to the cluster.

2.3 Energy Scale

The jet energy can be obtained from the cluster energy through an appropriate correction factor. CDF has a complete set of pseudorapidity dependent correction factors, obtained by a detailed study of p-pbar data, test beam data and Monte Carlo simulations[5].

The definition of the jet energy (momentum) associated to a measured cluster is the total energy (momentum) of all the particles (leptons, mesons and baryons) exiting the primary vertex within a cone of fixed radius R = 0.7 centered on the axis of the measured cluster. The correction factor takes into account the detector effects only, like the calorimeter response and

the magnetic bending of the charged tracks. It should be pointed out that in this scheme no attempt is made to reconstruct the energy of the parton from which the jet originates. This "instrumental" jet definition is less model dependent than others and it will make less difficult the comparison of measurement with theoretical prediction when higher order QCD corrections will be added to the calculation.

At present we can compare data only with the leading order calculation, where the two final state parton momenta are the available quantities. The chosen jet definition depends on the cone size, while the leading order calculation does not because it is based on the two final state partons that have no size in the η–φ space. Only higher order calculations can reproduce the dependence of the measurement on the cone size[6,7]. With the used cone radius (R=.7) the energy inside the cone is in average smaller than the associated parton energy. These losses are due to the out of cone fragmentation and radiation.

The average energy lost out of cone has been studied as a function of the jet energy. The flux of energy around the jet axis as a function of φ is shown in fig. 1 for clean two jet events. The level of energy at 90° from the jets has been ascribed to the underlying event and not considered belonging to the hard scattering. The corresponding amount of average underlying energy included in the cone of radius 0.7 is subtracted to each cluster. This is a constant correction as a function of the jet P_t.

The energy excess over the underlying event and outside the cone radius in fig. 1, is defined as the 'out of cone' energy loss. A correction must be applied to approximate the parton energy. The effect of these losses is studied comparing the mass spectra obtained with and without the out of cone correction. The ratio between the two spectra is shown in fig. 2. The out of cone correction enhances the low mass cross section.

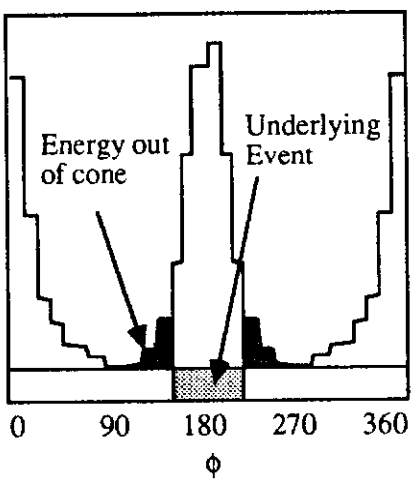

Fig. 1: Underlying event and out of cone energy in jet events

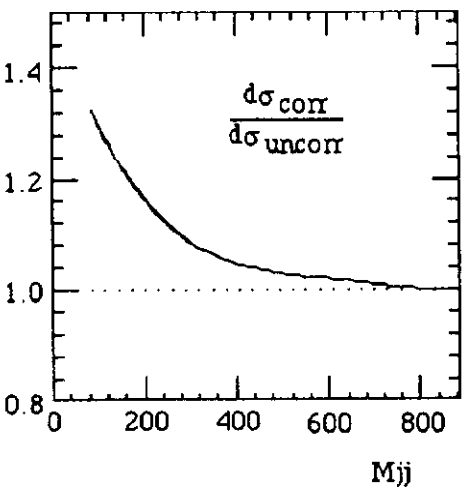

Fig. 2: Effect of the 'out of cone correction' on the mass spectrum

2.4 Event Selection

The criteria for the event selection are listed below.

a) $|Z_{vertex}| < 60$ cm; the longitudinal coordinate of the primary vertex was required to be within 60 cm from the center of the detector. This fiducial cut keeps the events inside the geometrical acceptance of the detector.

b) $|\Delta\varphi| < 30°$; the two leading jets were required to be back to back within 30° in the transverse plane. This is a loose cut to select two jet events.

c) $|Y_1| < 0.7$, $|Y_2| < 0.7$; the cross section was integrated over this rapidity region where Y_1 and Y_2 are the rapidities of the two leading jets in E_t. This cut also implies that both jets are measured by the central calorimeter.

2.5 Results

The invariant mass was calculated as $M_{jj} = [(E_1+E_2)^2 - (\mathbf{P}_1+\mathbf{P}_2)^2]^{1/2}$, where E_i and P_i are the measured energies and momenta of the two leading jets. Fig. 3 shows the plot of the differential cross section $d\sigma/dM_{jj}$ as a function of the dijet invariant mass M_{jj}. The dots represent the experimental points with their statistical errors. The underlying event correction and the out of cone correction were applied. It should be noted that the measurement extends over a range of nearly 6 orders of magnitude. The relative systematic error[8] on the cross section is roughly constant with the mass and of the order of 35%.

3. COMPARISON WITH THEORY

3.1 QCD Leading Order

The two dashed lines in fig. 3 define a band of uncertainty in the theoretical prediction. The theory has been smeared with the detector resolution[9] to be compared with the uncorrected data.

To obtain the theoretical band we calculated the predictions for the $2 \rightarrow 2$ QCD diagrams, varying the Q^2 within the range $0.5\ P_t^2 < Q^2 < 2\ P_t^2$ and using different parametrizations for the structure functions, namely EHLQ1, EHLQ2, DO1, DO2[2,10]. The band in fig. 3 is the envelope of all the predictions for different Q^2 and structure functions.

It should be noted that these QCD predictions refer to the leading order QCD matrix element and do not take into account gluon radiation from the initial and final state partons.

To have a more quantitative test of QCD, we fit on our data the theoretical predictions obtained changing structure functions and Q^2 scale. Since both data and theory have a normalization uncertainty, the free parameter of the fits was a global normalization factor. We used the statistical error only. The systematic error is still to be included in the fit before getting a conclusion, but it is already possible to observe that our spectrum is sensitive to differences between structure functions.

Both spectra with and without out of cone correction where used to test the theory. For

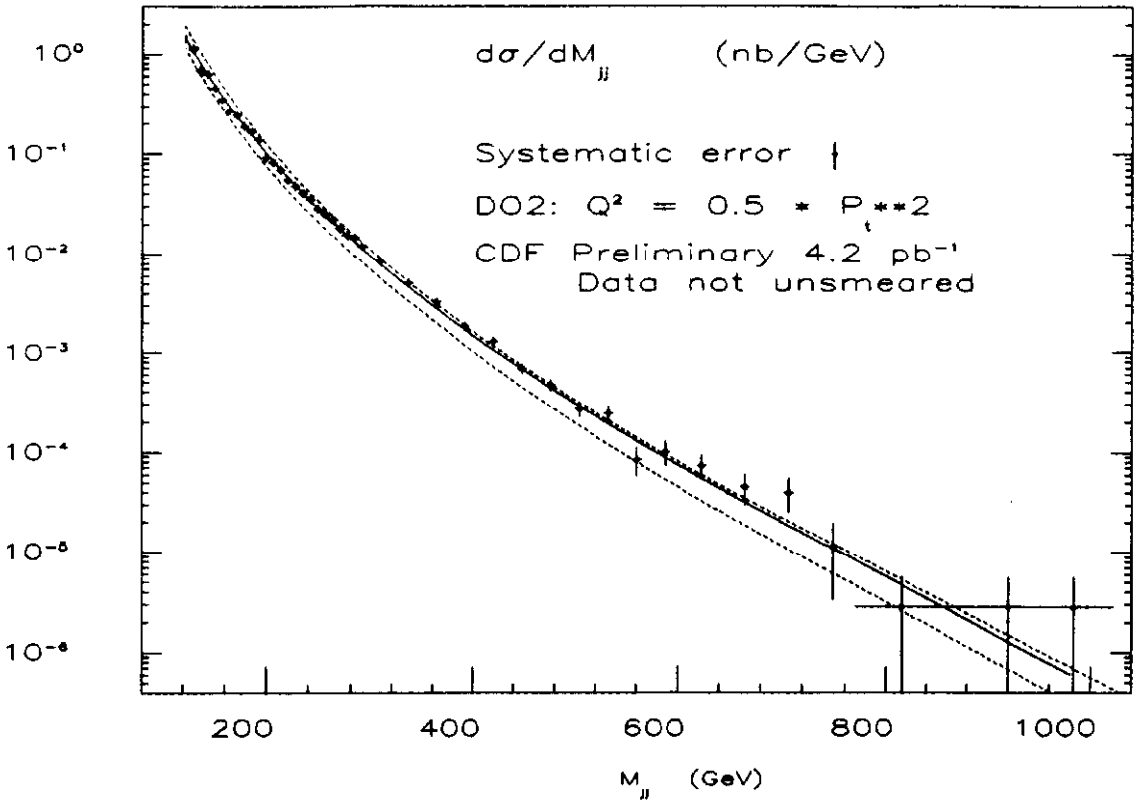

Fig. 3: Dijet Mass Spectrum

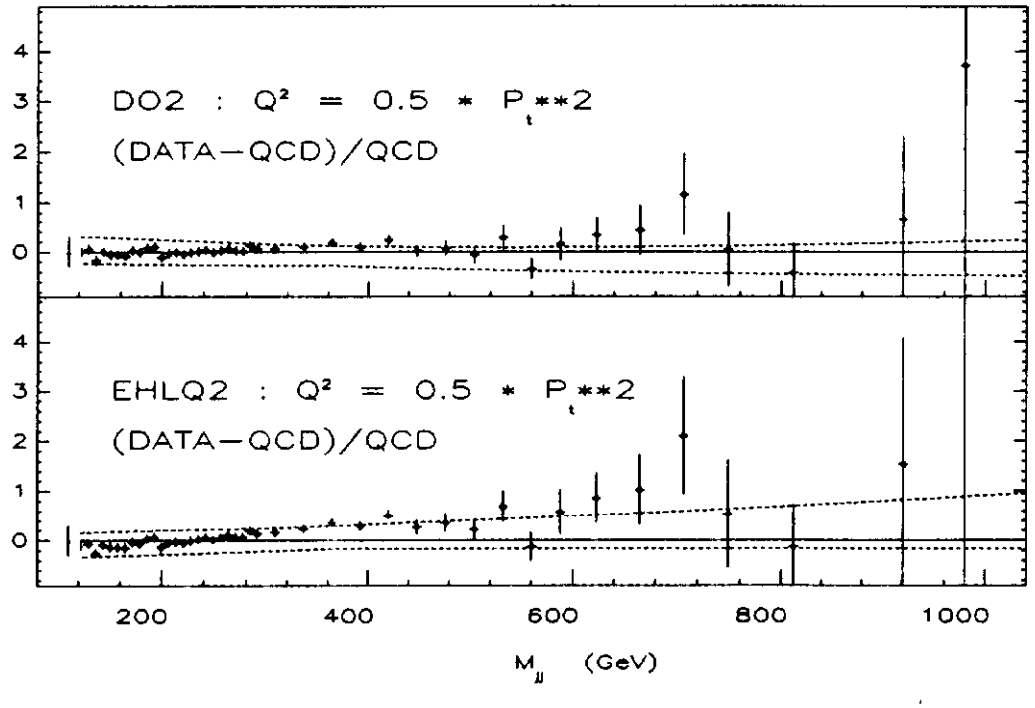

Fig. 4: Predictions from different Structure Functions

each theoretical choice, the spectrum with the out of cone correction shows a better agreement with the theory since it reproduces better the steep shape of the theory. DO2 with $Q^2=0.5\ P_t^2$ shows the best agreement with the data in terms of χ^2. The solid line of fig. 3 is the result of this fit. The worse agreement with the data is given by the structure function EHLQ2. The difference between the two fits is shown in fig. 4 on linear scale. The quantity (Data-QCD)/QCD is plotted as a function of the dijet mass. The dashed lines represent the same theoretical band shown in fig. 3 and the bar on the left side shows the size of the average systematic error.

3.2 Compositeness

To get a feeling for the sensitivity of the mass spectrum to the compositeness of the quarks, we fitted on the data the predictions obtained adding an effective 4-quark contact interaction[2] to the standard QCD lagrangian. Fig. 5a shows the prediction for different values of the compositeness energy Λ^*; as $\Lambda^* \rightarrow \infty$ the prediction approaches the pure QCD calculation. At energies less than the compositeness scale, a possible structure should show up as an increase of cross section at high masses. The curves are calculated at fixed $Q^2 = P_t^2$ and using the structure function DO2. Fig. 5b, c and d show the same fits on linear scale. This data confirm the present CDF limit of $\Lambda^*= 950$ GeV and an improvement of this limit is expected when the systematic error will be included in the fit.

4. QCD RADIATION

4.1 Effect of Radiation

As we said, a direct comparison of the measured mass spectrum with the $2 \rightarrow 2$ QCD calculation does not include the possibility of gluon radiation which generates secondary jets.

To measure the effect of the radiation on the cross section we added the non-leading jets in the computation of the invariant mass, whenever the distance (in η-φ space) from one of the leading jets was smaller than a fixed radius R_{cut}. The cut is intended to reject the jets generated by initial state radiation, which are likely to be away from the directions of the final state partons. We then looked at the dependence of the mass spectrum on the value of R_{cut}.

Fig. 6 shows how the cross section changes as R_{cut} changes. This figure shows, for different values of the sum cone radius R_{cut}, the ratio of the mass spectrum with the jet merging to the mass spectrum of the two leading jets. The effect grows up to a factor 1.7 for a radius $R_{cut} = 1.5$. The ratio is roughly costant as a function of the mass. This means that the radiation affects the absolute scale of the cross section more than the shape of the distribution.

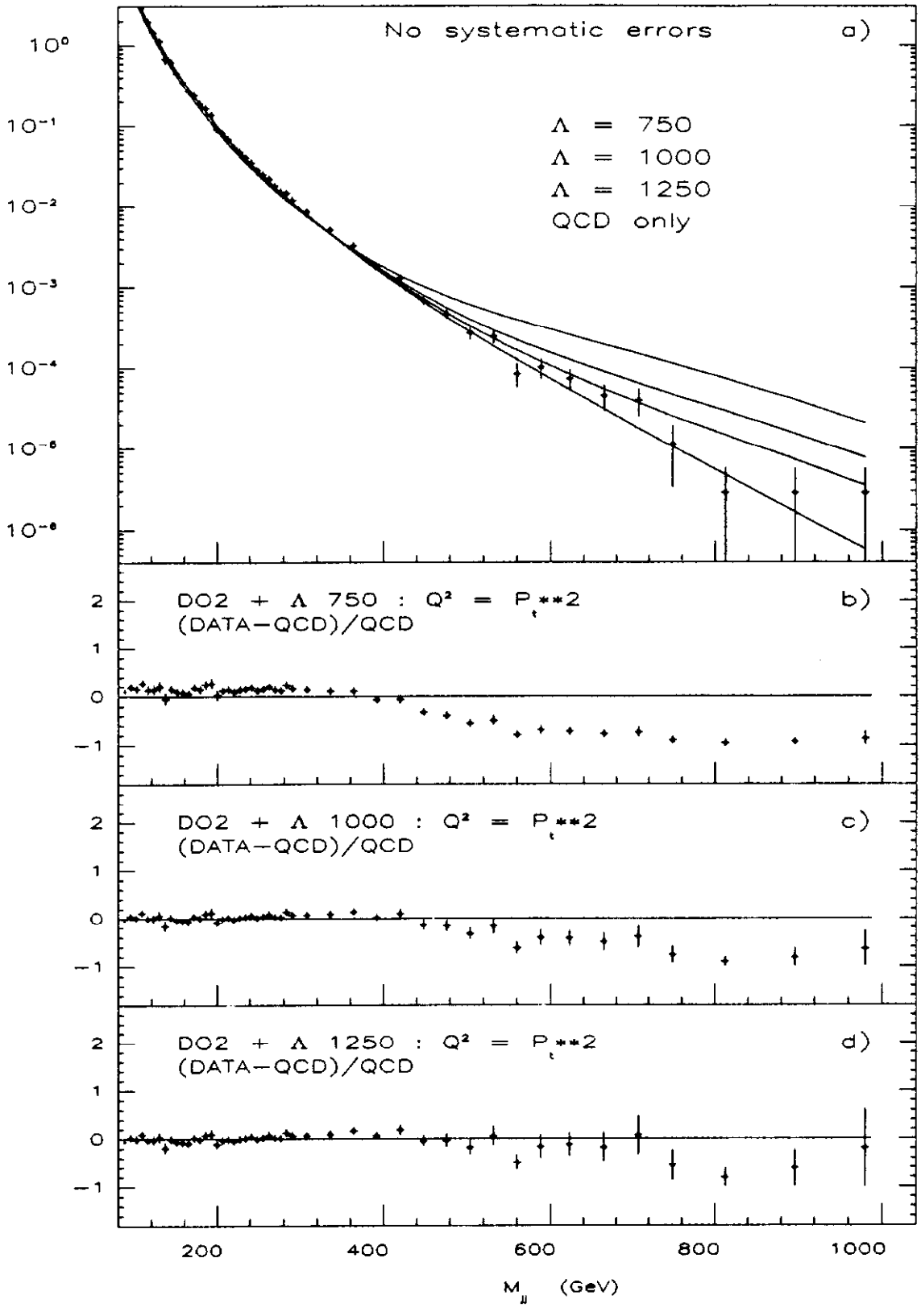

FIG. 5: Predictions from different Compositeness Scales

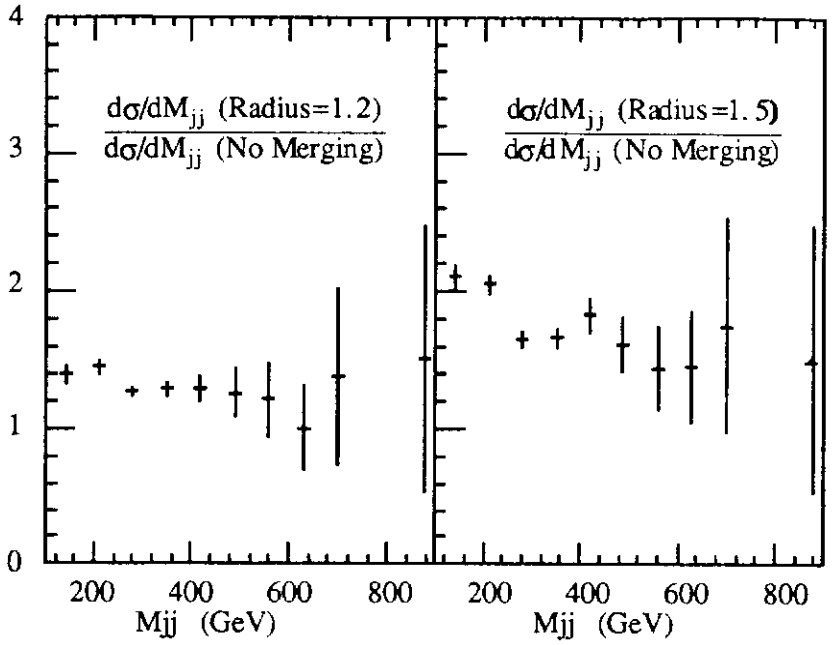

Fig. 6: Effect of the jet merging procedure on the mass spectrum

5. CONCLUSIONS

a) We measured the differential cross section $d\sigma/dM_{jj}$ as a function of the invariant mass M_{jj}.

b) A first comparison to the theoretical predictions shows that data are in agreement with the $2\rightarrow2$ QCD calculations, and that the mass spectrum is sensitive to differences between structure functions. Further analysis is under way to test MRS and DFLM structure functions and to give a quantitative limit for quark compositeness. The systematic error must be included in the procedure of fitting the theory on the data.

c) The mass spectrum is more exclusive than the E_t spectrum and it is more sensitive to the details of the QCD radiation, allowing a deeper probing of theoretical predictions.

e) We have in progress detailed tests on possible structures in the mass spectrum to give limits on the axigluon mass and to search for bumps, using cuts that enhance the resolution.

REFERENCES

1) F. Abe et al., Nucl. Instr. and Meth. **A271** (1988) 387
2) E. Eichten et al., Rev. Mod. Phys. **56** (1984) 579
3) P.H. Frampton and S.L. Glashow, Phys. Lett. **B190** (1987) 157
4) D. Brown et al., CDF Internal Note **605** (1988)
5) D. Brown and R. Carey, CDF Internal Note **755** (1988)
6) S.D. Ellis et al., Phys.Rev.Lett. **62** (1989)726; Phys.Rev.D **40**(1989)2188;
7) F.Aversa et al., Phys.Lett. **210B** (1988)225; **211B** (1988)465; Nucl.Phys. **B327**(1989)105
8) M. Dell'Orso et al., CDF Internal Note **1057** (1989)
9) M. Dell'Orso et al., CDF Internal Note **1056** (1989)
10) D. Duke and J. Owens, Phys. Rev. **D30** (1984) 49